Capacitive Wireless Powering for Electric Vehicles with Near-Field Phased Arrays

José Estrada [1], Sreyam Sinha, Brandon Regensburger, Khurram Afridi, Zoya Popović

Electrical Engineering Department, University of Colorado Boulder
425 UCB, Boulder, CO 80309 USA
[1] jose.estrada@colorado.edu

***Abstract*—This work demonstrates a simple approach for mitigating the high fringing electromagnetic fields produced by high-frequency capacitive wireless powering of electric vehicles. A 6.78 MHz (ISM band) single module Capacitive Wireless Power Transfer (CWPT) system based on GaN on Si inverters and rectifiers provides an output power of 110 W with an efficiency of 90%. The electric field produced by the single module is measured to be above the safety exposure limits provided by ICNIRP, consistent with previously reported CWPT. To reduce the E-field produced, while maintaining the required power transfer, a multi-module approach is introduced in which the separate modules are phased to provide a measured field reduction of over 24% and 43% for two and four module systems, respectively.**

I. Introduction

Electric vehicles (EV) are one of the most promising substitutes for internal combustion engine vehicles (ICEV). EVs have greater well-to-wheel efficiency than ICEVs and since their global market share remains under 1%[1] there is a great necessity for innovation. Although advances are made in battery technology (particularly Lithium-ion) and charging systems [2], [3], many problems related to greater EV penetration remain to be solved. One of the challenges is the short driving range of EVs compared to ICEVs. A typical ICEV has a range of about 500 km while a typical EV has on average about 150 km of range and the highest values are around 450 km for the higher-end EVs [4]. One of the possible solutions to this problem is wireless powering of the EV in motion on the road, which also reduces battery requirements. Power transfer on the order of 20 kW can be used to power an EV at cruising speeds and is usually the design specification for these systems [5]. Additionally, WPT is an attractive alternative for charging EVs in parking lots, garages and other static scenarios where a wireless system can prove to be more convenient and reliable.

So far efforts have been made to demonstrate wireless power transfer to electric vehicles using inductive power transfer, e.g. [5], [6], [7], and a few limited cases of capacitive power transfer, as in [8], [9]. Our goal is to develop a CWPT System that can provide 50 kW over a 12 cm gap using an area of less than 1 m^2 with an efficiency above 90%. Figure 1 shows the overall geometry for Wireless Power Transfer (WPT) to an EV with a capacitive near field phased array. CWPT has several advantages over inductive WPT systems: (1) does not require the use of heavy and expensive ferrites for field concentration; (2) benefits from higher frequencies of operation since the capacitive reactance between the vehicle and the road is inversely proportional to frequency; (3) the displacement current corresponding to high power transfer requires a lower electric field at higher frequencies; and (4) sensitivity to misalignment is reduced using an appropriate geometry [8].

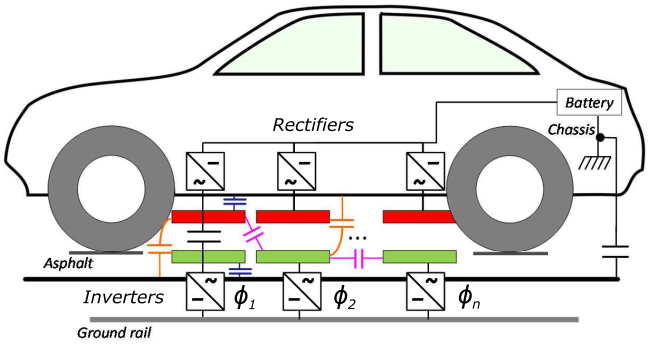

Fig. 1. Overall geometry for capacitive wireless powering in electric vehicles, showing multiple phased CWPT modules that consist of an inverter in the road, and a pair of capacitive plates and a rectifier in the vehicle that charges the on-board battery. Parasitic capacitances from plates to chassis, plate to road-rail, chassis to road-rail and between adjacent plates are also shown.

Due to the large electromagnetic fields that are associated with high power transfer, safety is an important issue that remains to be solved. Exposure limits like the ones found in [10] restrict the electromagnetic fields that humans can be exposed to, and these must be met for any product commercialization. Approaches to fringing field reduction using near-field phased arrays of inductive [11], [12] and capacitive [13] powering modules have been previously attempted. This paper expands on the work of [13] by validating the multi-modular approach with measurements of both the field produced by a single module and the effect of using a near-field phased array.

The paper is organized as follows: section II deals with the design and performance of a single CWPT module; in section III the multi-module system is explained and simulations are shown; and measurement results are displayed in section IV.

II. Single Module Design

A photograph of a single module in the CWPT system is shown in Figure 2, with the corresponding circuit diagram in Figure 3. The inverter has an H-bridge topology and is

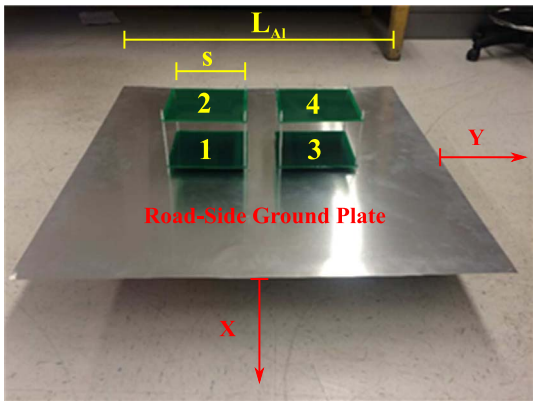

Fig. 2. Single module photograph showing the four capacitive plates. The top aluminum sheet that models the vehicle has been removed for visibility. The side length of the aluminum sheet is L_{Al} =100 cm. The red arrows indicate the two measurement locations.

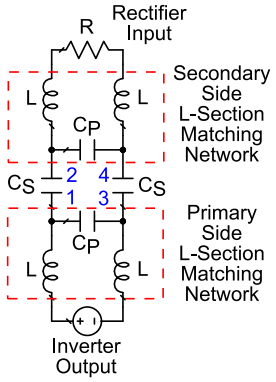

Fig. 3. Equivalent circuit of the CWPT system including the L-section matching networks. C_S and C_P represent the effective capacitive coupling of the CWPT system.

implemented with 650 V, 15 A GaN on Si FETs (GaNSystem GS66504B). The frequency of operation is 6.78 MHz (ISM band). This module transfers power through a pair of coupling plates, one in the forward path and one in the return path. To minimize circulating current and enable soft-switching in the inverters, it is desired to have a near-resistive input impedance. Therefore, compensation is required and is implemented using L-section matching networks at the primary and secondary side, designed to achieve high efficiency by the method proposed in [14].

In order to mimic a practical vehicle charging system, aluminum sheets are added above and below the coupling plates to model the vehicle and the road, as shown in Figure 2, where the top aluminum sheet has been removed for visibility. The equivalent π circuit model for the various capacitances between the charging plates and road/car sheets is shown in Figure 1. The primary and secondary side matching networks are then designed to transfer power through the equivalent series capacitances of this π-network and the parallel capacitances are absorbed into the L-section matching networks as shown by the equivalent circuit in Figure 3.

The experimental system has square plates with a side

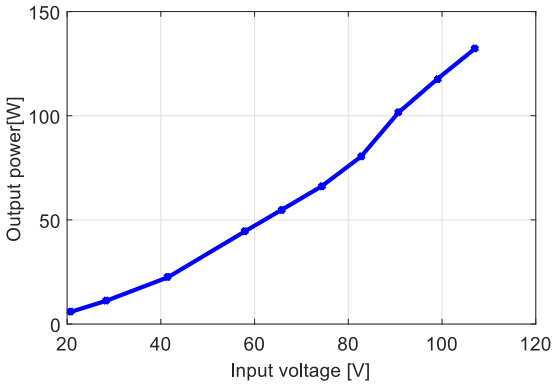

Fig. 4. Measured output power of the single module system with versus input DC voltage. Output powers above 110 W correspond with 90% efficiency.

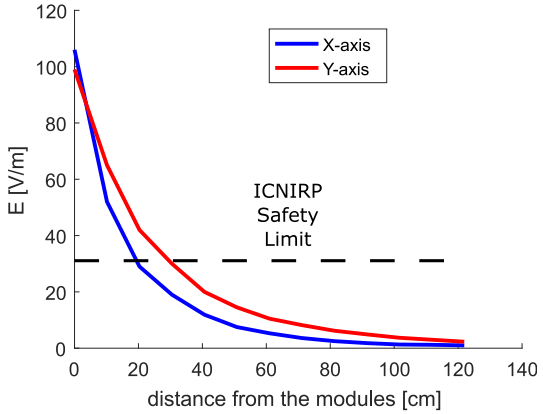

Fig. 5. Measured electric field magnitude (RMS) of the single-module CWPT system. The distance references are the edges of the ground plane, which can be seen in Figure 2. The origin corresponds to the edges of the aluminum sheet.

s =17.68 cm, and the L-section matching network has a parallel capacitance C_S =14.2 pF, a series capacitance C_P =0.8 pF and series inductors L =22.4 μH designed according to [14]. The prototype provides 110 W of output power with an efficiency of 90% to an RF load R =42 Ω that simulates the input of the rectifier. Figure 4 shows the measured output power as a function of input DC voltage.

III. Multi-module System

The total magnitude of the electric field vector inside and around the vehicle, where people may be present, has to be below the limits set by the International Commission on Non-Ionizing Radiation Protection (ICNIRP) [10]. The electric field produced by the single-module prototype is shown in Figure 5. The fields exceed the ICNIRP safety limit of 33.4 V/m (RMS) at 6.78 MHz and will increase as the output power increases to the required kW levels.

To comply with the exposure limits in [10], the field must be reduced. To this end we use a multi-module CWPT system, with the architecture as simulated in [13] and shown in Figure

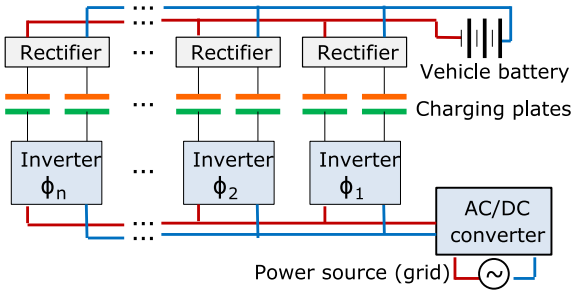

Fig. 6. Block diagram of a multi-module CWPT system, with receiving-side capacitor plates shown in orange, and road-side plates shown in green. Phase shifts are applied within the inverters in order to reduce the fringing fields and meet safety requirements.

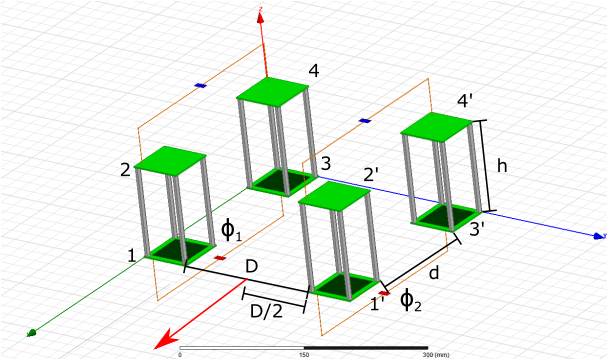

Fig. 7. HFSS simulation setup, where a 50 V voltage source (red) is used on the inverter side (bottom), and the rectifier side is prepresented with a 2 kΩ (blue) load. The plates are printed on the green FR4 substrate and the gray dielectrics are nylon standoffs. The red arrow references the location where the field is measured. The plates denoted with 1', 2', etc. belong to the second module.

6. The near field reduction is achieved by a relative phase between adjacent identical modules, analogous to beam steering in the far field of phased array antennas. In [13] it is shown by full-wave simulations that the optimum field cancellation is obtained when the phase shift is 180°, making the feeding of the modules very simple, as long as the feeding is done in a balanced way. Full-wave EM simulations of the CWPT system with plate geometry corresponding to the measured module were performed using ANSYS HFSS, Figure 7 shows the setup used for the simulations.

IV. Field Cancellation Measurements

Figure 8 shows a photograph of a two-module experimental setup used to measure the electric field generated by the parallel plate CWPT modules. The plates are 5 cm×5 cm in size and with separations of $h = 12$ cm between plates and $d = 15$ cm between pairs of plates of the same module. The modules are located at a distance $D = 20$ cm from each other. A load resistance of 2 kΩ represents the input of the secondary side L-section matching network loaded with the rectifier. The feeding signal is generated using an RF transmitter to emulate the output of the inverter and provide a reasonably high power level. The plates are fed with a 50 V peak sine wave generated by a ICOM IC-7410 frequency locked RF

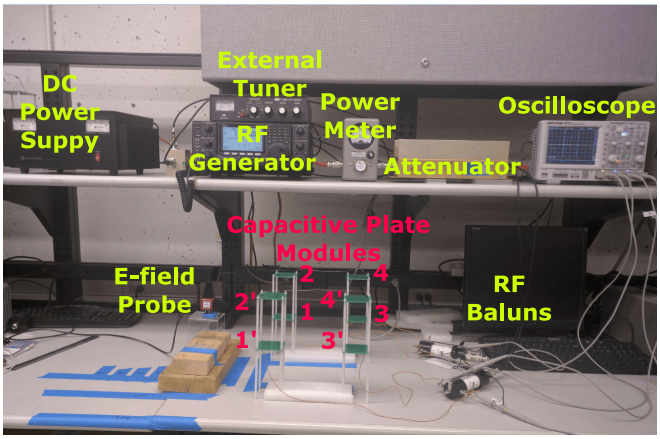

Fig. 8. Multi-module CWPT system photograph, showing 8 plates corresponding to 2 modules, as well as the E-field probe and baluns used to provide out-of-phase feeding.

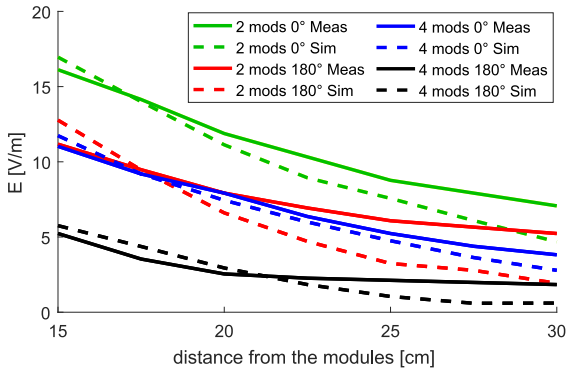

Fig. 9. E-field measurement (solid) and simulations (dashed) at 7 MHz as a function of distance along x axis for two modules (green and red), four modules (blue and black), and different phases.

transmitter at 7, 14 and 29 MHz. These frequencies are within amateur radio designated bands and are selected because of amplifier availability and proximity to the ISM bands (6.78, 13.56 and 27.2 MHz). The voltage applied to the plates is monitored using an oscilloscope with differential probing. The electric field is measured using an ETS HI-6005 electric field probe. The plates are fed using high-power baluns (W2AU) to ensure balanced feeding of the modules.

Figures 9, 10 and 11 show the electric field as a function of distance from the CWPT system at three ISM band frequencies for 2 and 4 modules and for different relative phases between modules. Figure 12 shows the field reduction computed as

$$\Delta E = \frac{E_{0^\circ} - E_{180^\circ}}{E_{0^\circ}} \times 100$$

where E_{0° and E_{180° are the magnitudes of the electric field generated by the system when the feeding is done in phase and with phasing of 180°. The field reduction is above 24% for the two-module system and 32% for the four-module system at three frequencies. At closer distances (less than 25 cm), where the fields are more intense, the reduction is above 24% and

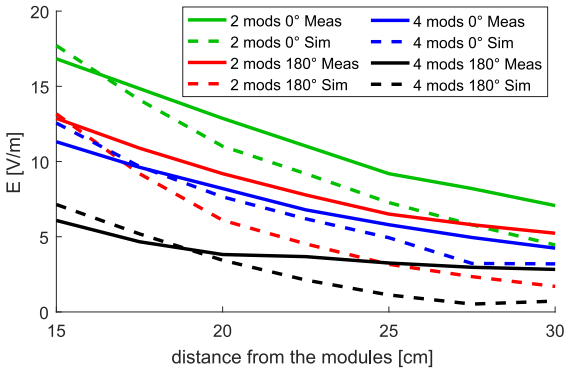

Fig. 10. E-field measurement (solid) and simulations (dashed) at 14 MHz as a function of distance along x axis for two modules (green and red), four modules (blue and black), and different phases.

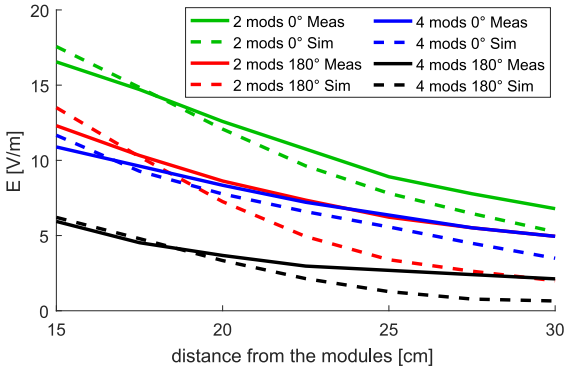

Fig. 11. E-field measurement (solid) and simulations (dashed) at 29 MHz as a function of distance along x axis for two modules (green and red), four modules (blue and black), and different phases.

43% for the two and four module systems, respectively. The results of the simulations diverge from the measurements at larger distances due to the decreased sensitivity of the field measurement at lower field strengths and lack of modeling of surrounding objects.

V. Conclusion

In this work we have demonstrated a method for reducing fringing electric fields in a capacitive WPT system using a near-field phased array consisting of multiple CWPT modules. Field reduction of 24% with a two-module system and 43 % with a four-module system, at distances closer than 25 cm and for frequencies of 7, 14 and 29 MHz. Full-wave EM simulation trends agree well with measurements and any deviations can be attributed to lack of modeling of the surroundings.

Acknowledgment

The authors wish to acknowledge Katharine Doubleday, Ashish Kumar and the financial support received from the Advanced Research Projects Agency-Energy (ARPA-E), U.S. Department of Energy, under the Award Number DE-AR0000618.

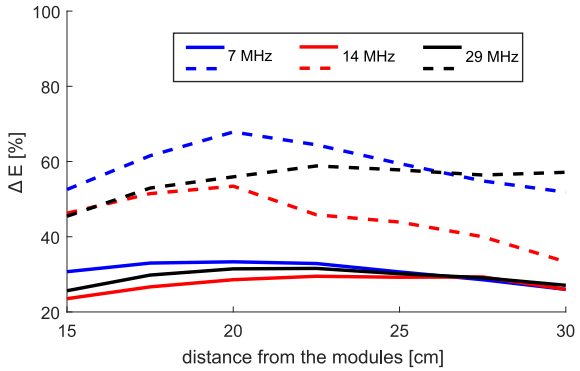

Fig. 12. Two and four module systems electric field difference (ΔE) between the 0° and the 180° phase shifted feed; the solid and dashed traces correspond to the two and four module systems, respectively.

References

[1] http://www.ev-volumes.com/country/total-world-plug-in-vehicle-volumes/, accessed: 2017-02-10.

[2] S. S. Williamson, A. K. Rathore, and F. Musavi, "Industrial electronics for electric transportation: Current state-of-the-art and future challenges," *IEEE Transactions on Industrial Electronics*, vol. 62, no. 5, pp. 3021–3032, May 2015.

[3] P. Miller, "Automotive lithium-ion batteries: State of the art and future developments in lithium-ion battery packs for passenger car applications," *Platinum Metals Review*, vol. 59, no. 1, pp. 4 – 13, 2015.

[4] W. Kempton, "Electric vehicles: Driving range," *Nature Energy*, Aug. 2016. [Online]. Available: http://dx.doi.org/10.1038/nenergy.2016.131

[5] G. A. Covic and J. T. Boys, "Modern trends in inductive power transfer for transportation applications," *IEEE Journal of Emerging and Selected Topics in Power Electronics*, vol. 1, no. 1, pp. 28–41, March 2013.

[6] S. Y. R. Hui, W. Zhong, and C. K. Lee, "A critical review of recent progress in mid-range wireless power transfer," *IEEE Transactions on Power Electronics*, vol. 29, no. 9, pp. 4500–4511, Sept 2014.

[7] J. Enriquez, "Qualcomm wireless technology charges electric vehicles in motion," https://www.rfglobalnet.com/, accessed: 2017-05-19.

[8] H. Zhang, F. Lu, H. Hofmann, W. Liu, and C. C. Mi, "A four-plate compact capacitive coupler design and lcl-compensated topology for capacitive power transfer in electric vehicle charging application," *IEEE Transactions on Power Electronics*, vol. 31, no. 12, pp. 8541–8551, Dec 2016.

[9] J. Dai and D. C. Ludois, "Capacitive power transfer through a conformal bumper for electric vehicle charging," *IEEE Journal of Emerging and Selected Topics in Power Electronics*, vol. 4, no. 3, pp. 1015–1025, Sept 2016.

[10] I. C. on Non-Ionizing Radiation Protection (ICNIRP), "Guidelines for limiting exposure to time-varying electric, magnetic and electromagnetic fields (up to 300 ghz)," *Health Physics*, vol. 74, no. 4, pp. 494 – 522, 1998.

[11] B. H. Waters, B. J. Mahoney, V. Ranganathan, and J. R. Smith, "Power delivery and leakage field control using an adaptive phased array wireless power system," *IEEE Transactions on Power Electronics*, vol. 30, no. 11, pp. 6298–6309, Nov 2015.

[12] G. Sauerlaender and E. Waffenschmidt, "Wireless power transmission system," Aug. 19 2014, uS Patent 8,810,071. [Online]. Available: https://www.google.ch/patents/US8810071

[13] I. Ramos, K. Afridi, J. A. Estrada, and Z. Popovic, "Near-field capacitive wireless power transfer array with external field cancellation," in *2016 IEEE Wireless Power Transfer Conference (WPTC)*, May 2016, pp. 1–4.

[14] S. Sinha, A. Kumar, S. Pervaiz, B. Regensburger, and K. K. Afridi, "Design of efficient matching networks for capacitive wireless power transfer systems," in *2016 IEEE 17th Workshop on Control and Modeling for Power Electronics (COMPEL)*, June 2016, pp. 1–7.